


Influence of Brazing Technology on the Microstructure and Properties of YG20C cemented carbide and 16Mn steel joints

Yanwei Sui¹ · Haibo Luo¹ · Yang Lv¹ · Fuxiang Wei¹ · Jiqui Qi¹ · Yezeng He¹ · Qingkun Meng¹ · Zhi Sun¹ 

Received: 30 May 2015 / Accepted: 25 July 2016 / Published online: 2 August 2016
© International Institute of Welding 2016

Abstract Cu-Mn-Zn brazing filler metal was used to study the vacuum brazing of YG20C cemented carbide and 16Mn steel. Then the effects of brazing temperature on the structural properties and element distribution at joints were explored separately through scanning electron microscopy (SEM), energy disperse spectroscopy (EDS) and three-point bending test. The results showed that Cu-Mn-Zn brazing filler metal can efficiently wet both YG20C cemented carbide and 16Mn steel. The bending strength of the seam was maximum at the temperature of 960 °C and at the brazing filler metal thickness of 0.2 mm.

Keywords Brazed joints · Vacuum · Brazing · Carbides · Carbon manganese steels

1 Introduction

Cemented carbide is made of hard compound and binder metal by powder metallurgy technology. With high hardness, wear resistance, heat resistance and corrosion resistance, cemented carbide is hailed as “industrial teeth”. Because of these advantages, it is widely used to prepare hard cutting tools and wear-resistant parts, which has significant influence on mechanical processing, geological prospecting, mining and other industrial fields. However, the prime cost is

unacceptable, so many researchers devote themselves to research hard alloy/steel composites. Hongsheng Chen et al [1, 2] researched the brazing between a functionally graded WC-Co/Ni component and 410 stainless steel with Cu-Zn brazing filler metal. By analyzing the brazing joint, they found (Cu, Ni)-based solid solution was formed between the brazing and Ni layer, which contributed to relaxing stresses and improving the strength of the cemented carbide/stainless steel joints. Liu Zhu et al [3] firstly applied electroless plating to prepare Ni-Cu-P layer on the surface of YT15 cemented carbide, and then brazed it on steel-base. The results showed that the electroless plating Ni-Cu-P layer apparently improves the brazability of cemented carbide to steel. And under optimal conditions: the concentration of copper sulfate (CuSO₄) is 1.25 g/L, pH value is 11, and plating temperature is 90°C, the brazability reached the best, the shear strength of copper brazing joint is up to 480 MPa. Chen Guoqing et al [4] directly brazed WC-Co hard alloy and SAE1045 steel by electron beam. Finite element analysis of the brazing sequence indicated that the maximum residual stress distributed at the brazing joint or the hard alloy matrix metal where the macroscopic cracks tended to generate. According to the metallurgical compatibility principle, the cracks can be avoided by a powder metallurgy Ni-Fe intermediate during electron beam welding–brazing of hard alloy to steels. Yaoita et al [5] studied the reason for the improvements in the wetting characteristics due to the presence of the Ni element in Ag-Cu-Zn brazing filler metal, as well as the effects of the Ni element on the bending strength of the brazing joints. The results showed that by adding the Ni element, α -Cu solid solution phases were formed in the brazed layer along the interface. Consequently, the distribution of Ag and Co elements across the interface between cemented carbide and α -Cu solid solution phases varied continuously, which caused the wetting characteristics to improve. They also found the addition of the Ni element decreased the bending strength

Recommended for publication by Commission C-XVII - Brazing, Soldering and Diffusion Bonding

✉ Zhi Sun
D_Robinhood@126.com

¹ School of Materials Sciences and Engineering, China University of Mining and Technology, Xuzhou 221116, China

of the brazed joint by expanded the Co depleted zone. Patricio F. Mendez et al [6] deposited the Ni-base with the addition of tungsten carbide particles on the Fe-base as wear resistant overlays by oxy-acetylene flame brazing. The results showed that the microstructure was Co-Cr matrix alloy, in which dissolved some long dark rod-like chrome-rich primary carbides phases that provided the high abrasion resistance to the overlay. Moreover, many researchers did much in-depth study on cemented carbide brazing, and got a lot valuable results [7–16]. In recent years, the domestic research on brazing of cemented carbide and steel are mostly concentrated on vacuum brazing, considering that the vacuum brazing can avoid the oxidation of brazing filler metal and matrix metal. On this basis, our team probe into the vacuum brazing process between YG20C cemented carbide and 16Mn steel based on Cu-Mn-Zn brazing filler metal. In addition, we analyze the microstructure and properties of the joints to make sure the optimum brazing process. And there is no doubt that the experiment has certain reference significance to the research of brazing technology of cemented carbide and steel.

2 Materials and methods

Table 1 showed the main parameters of the base materials (YG20C cemented carbide and 16Mn steel) and the brazing filler metal (Cu-Mn-Zn).

The base materials in the brazing tests were processed into cuboid specimens ($17 \times 17 \times 5 \text{ mm}^3$, brazing surface $5 \times 17 \text{ mm}^2$). The brazing filler metal was cut into sheets with the dimensions lightly larger than the brazing surface, about $8 \times 20 \text{ mm}^2$, which guaranteed that the brazing filler metal was sufficient to fill in the brazing gaps. The brazing filler metal was ground bright with sand paper to remove the oxide layer. All polished materials were immersed in acetone for 5–10 min, then cleaned up and dried. Finally, the brazing filler metal was placed between the cemented carbide and the 16Mn steel. The seam gaps were controlled by placing round molybdenum wires at two edges of each seam (Fig. 1). Then the brazing specimens were placed into a special fixture and fixed and pressed with heat-resistant steel ($\sim 250 \text{ g}$) as loading pieces. After that, the specimens were put in a vacuum sintering furnace. The vacuum degree was maintained at about $5 \times 10^{-2} \text{ Pa}$ during the heating and cooling.

Table 1 Chemical composition of the materials using in the experiment

	Component (%)						
	WC	Co	C	Si	Mn	Fe	Cu Zn
YG20C	80	20					
16Mn			≤ 0.20	≤ 0.50	≤ 1.70	bal.	
CuMnZn					4		58 38

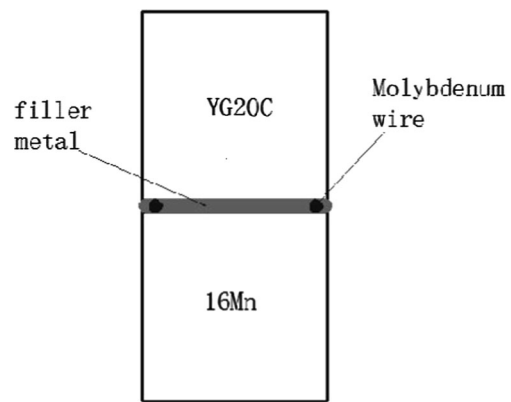


Fig. 1 The form of brazed joint

The melting temperature range of the brazing filler metal was $880\text{--}930 \text{ }^\circ\text{C}$ measured by differential thermal analysis (DTA). Thus, the brazing temperature in this experiment was set at $940\text{--}980 \text{ }^\circ\text{C}$, with an interval of $10 \text{ }^\circ\text{C}$. Then brazing tests were performed at the optimal brazing temperature to determine the optimal seam width. The heating process was that: raised from the room temperature at a rate of $10 \text{ }^\circ\text{C}/\text{min}$ to $880 \text{ }^\circ\text{C}$ and then maintained there for 30 min. After that, the temperature was raised at $10 \text{ }^\circ\text{C}/\text{min}$ to the predetermined level: 940°C , 950°C , 960°C , 970°C , 980°C , and maintained there for 15 min, followed by cooling along with the furnace (Fig. 2).

The wettability of brazing filler metal on base materials had significantly effect on brazed joint. In the wettability test, the specimen was plate shape, which had be removed the burr and washed with acetone. The size of the specimen and the location of the brazing filler metal were showed in Fig. 3. Remove the oxide film on brazing filler metal surface, next cut it into thin strips and roll it into granular with the balance of 150 mg. And then put it on the surface of $16.5 \times 16.5 \text{ mm}$ and locate it in the center of the specimen. The experiments were conducted on the BSD vacuum sintering furnace, and the last step was measuring the wetting angle using a goniometer.

After the brazing, the specimens were ground smooth, and were cut with a wire cutting machine into rectangular blocks

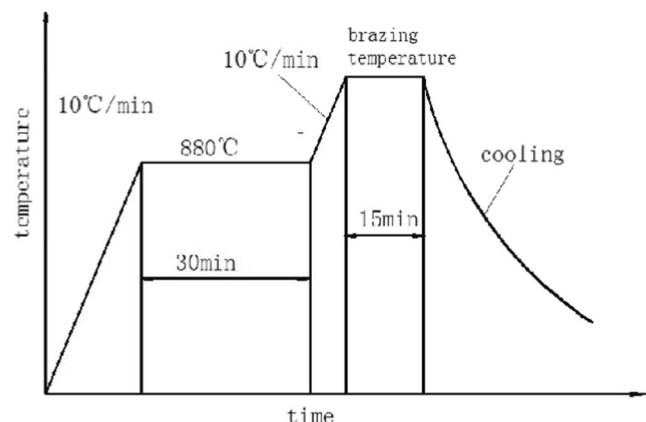


Fig. 2 The process curves of vacuum brazing

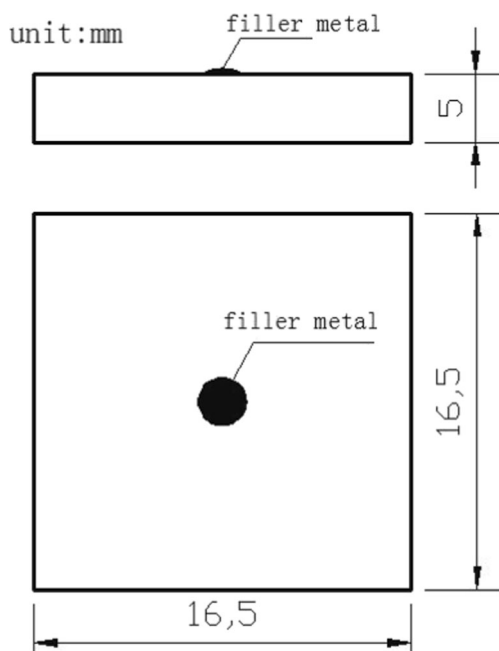


Fig. 3 The schematic diagram of wettability test

($5 \times 5 \times 34 \text{ mm}^3$), followed by the measurement of bending strength. The brazing seams at the side of the cemented carbide were corroded with a newly-prepared Murakamas reagent, and those at the side of the 16Mn steel were corroded with 3%-5% nitric acid alcohol solution, followed by microstructure analysis.

3 Results and analysis

3.1 wettability test

Fig. 4 displayed the results of wettability test for Cu-Mn-Zn brazing filler metal at different brazing temperature. Obviously, the wettings angles of Cu-Mn-Zn brazing filler metal on two parent metals were no more than 18 centigrade. This showed that the brazing filler metal had good wettability

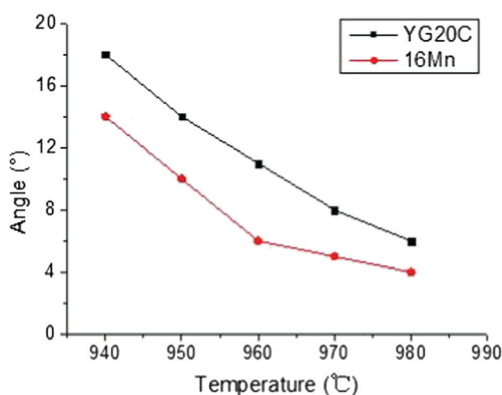


Fig. 4 The result of wettability test for Cu-Mn-Zn brazing filler metal at different brazing temperatures

for two parent metals: the YG20C cemented carbide and 16Mn steel. With the increase of brazing temperature, the wetting angles were apparently decreasing, and this made it clear that the wettability of brazing filler metal improved. At each brazing temperature, the wetting angle of the brazing metal on 16Mn steel was slightly smaller than that on the YG20C cemented carbide. It indicated that the wettability of brazing filler metal with 16Mn steel was better than that with the YG20C cemented carbide.

3.2 Microstructure analysis and Line scanning at brazing joints

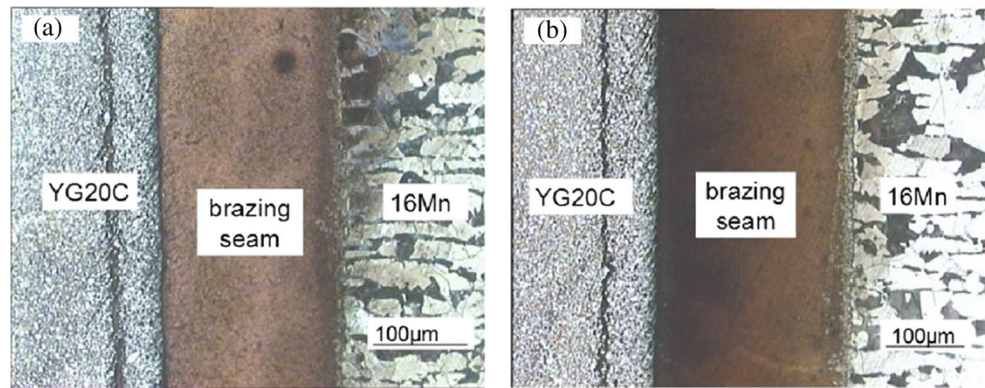
To investigate the structural properties of brazing seams, we analyzed the metallographic structure of the joints at different brazing temperatures. Fig. 5 showed the microstructures of the joints brazed at different temperature, and the Fig. 6 showed the microstructures of the interface brazed at 960 °C.

According to Fig. 5 and Fig. 6, we could see that the microstructures of the brazing joints were compact without any obvious brazing defects such as pores, inclusions, cracks, etc. The brazing seam combined with the base metal well, and the reaction zone was obvious in the interface of the brazing seam and the two base materials. The reaction zones near the YG20C cemented carbide were continuous thin strip, and along with the increase of the temperature, the changes in the reaction zones were not apparent. But the reaction zones near the 16Mn steel were complex and irregular, some of which were cobblestone-appearance. It was noteworthy that the reaction zones at 960 °C were largest, and the brazing filler metal had deeply embedded with the 16Mn steel. It showed that the metallurgical bonding between the brazing filler metal and the 16Mn steel was intense, which improved the mechanical properties of the joints.

To more accurately analyze the structural composition and element diffusion of the brazing joints, we did element line scanning for the joints formed at 960 °C. Fig. 7 was the line scanning result of the joint at 960 °C, and Table 2 is the EDS result of element content in interface of the joint at point A and B.

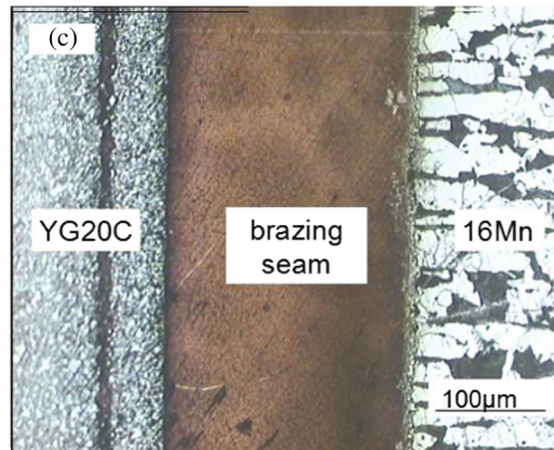
It could be seen from the linear scanning results that, the main elements in the center of the brazing seam were Cu and Zn formatting the Cu-Zn based solid solution. In the meantime, a little Cu and Zn also diffused into aside base materials. The saturated vapor pressure of Mn is high and it is active in vacuum atmosphere at high temperature, so a lot of Mn diffused into the aside base materials. The WC in the YG20C cemented carbide have high melting point, stable performance, and the bond between W and C cannot be destroyed even at very high temperature. So that only a little of W element dissolved into the brazing filler metal solution, and spread to the 16Mn steel. Fe and Co element made long-range diffusion to both sides through the brazing seam. In the reaction zones of the interface, there was apparent

Fig. 5 Microstructures of the joints brazed at different temperature



Microstructures of the joints brazed at 950°C

Microstructures of the joints brazed at 960°C



Microstructures of the joints brazed at 970°C

enrichment area of Fe and Co: near the YG20C cemented carbide, the content of Fe, Co was 20.62%, 46.75% respectively; and near the 16Mn steel the content of Fe, Co was 31.91%, 22.33% respectively. By Fe-Co phase diagram, Fe and Co can be infinitely miscible to form a solid solution, so we

concluded that most of interfacial reaction products were Fe-Co based solid solution, which also included Cu, Zn, Mn and other elements. This analysis indicated that the molten brazing filler metal could strongly combine the base materials by atomic diffusion.

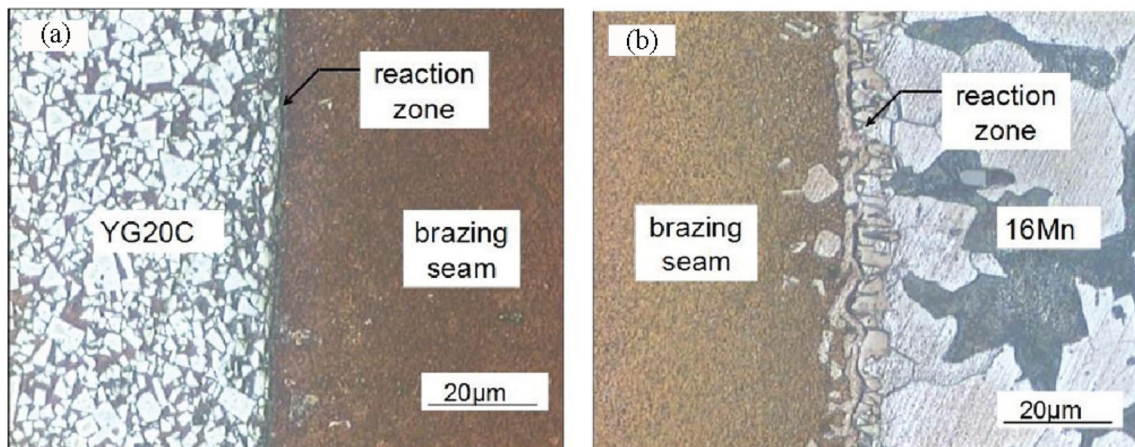


Fig. 6 Microstructures of the interface brazed at 960°C (a) YG20C (b) 16Mn

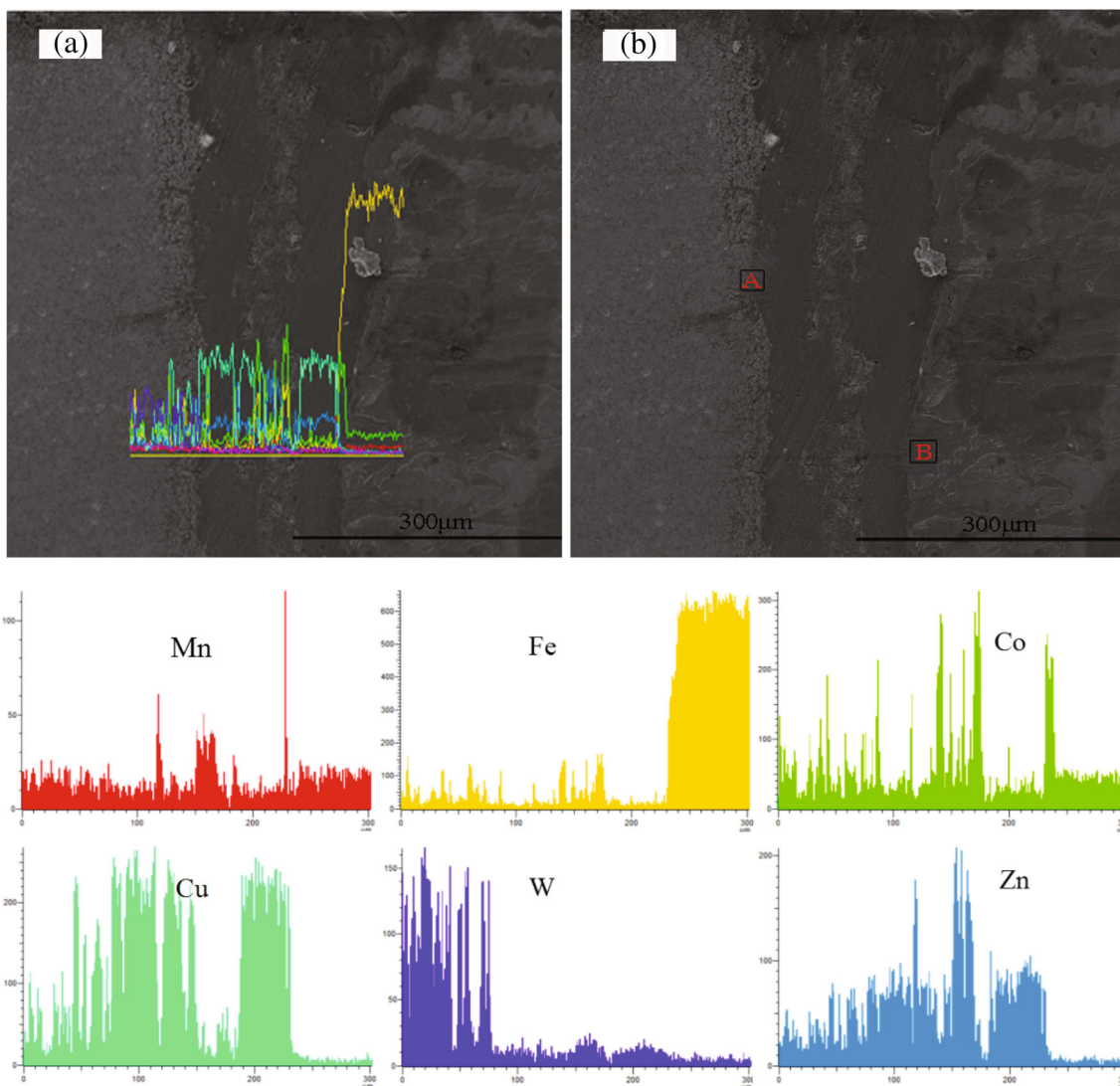


Fig. 7 (a) Linear scanning and (b) spot EDS of the joint at 960°C

3.3 Micro-hardness and Three-point bending test

Taking factors into consideration, we just measured the micro-hardness in the brazing seam and reaction zone near 16Mn, because the micro-hardness of cemented carbide cannot be measured accurately. In order to minimize the error, we measured three time in every sample, and the measurement points were selected in the area A and B showed in Fig. 8 (b). Table 3 and Fig. 8 (a) were the results of micro-hardness test for the joints brazed at different temperatures. It could be noticed that

the micro-hardness near 16Mn steel was higher than that in the brazing seam. This was mainly because much hard Fe-Co based solid solution was formed here, while a large number of soft Cu-Zn based solid solution was formed in the brazing seam. With the increase of brazing temperature, the micro-hardness in brazing seam did change-but not much; when it came to the micro-hardness near the 16Mn steel, it showed a rising trend owing to the diffusion of Fe, Co element and more Fe-Co based solid solution formed. This could exactly prove that the base materials have been strongly combined together by atomic diffusion.

Table 2 Point EDS results of element content in interface of the joint at point A and B(wt%)

	Mn	Fe	Co	Cu	Zn	W	Total
A (YG20C)	-0.17	20.62	46.75	11.36	6.43	15.01	100
B (16Mn)	0.11	31.91	22.33	28.92	16.04	0.68	100

The three-point bending test samples were processed into cuboid specimens (35×5×5 mm³), making the brazing joints on the centre of it. Table 4 showed the results of three-point bending tests at the joints at varying brazing temperature. Clearly, with the increase of brazing temperature, the bending strength at the joint was generally first enhanced and then weakened, and maximized at 960 °C. The joint ruptures

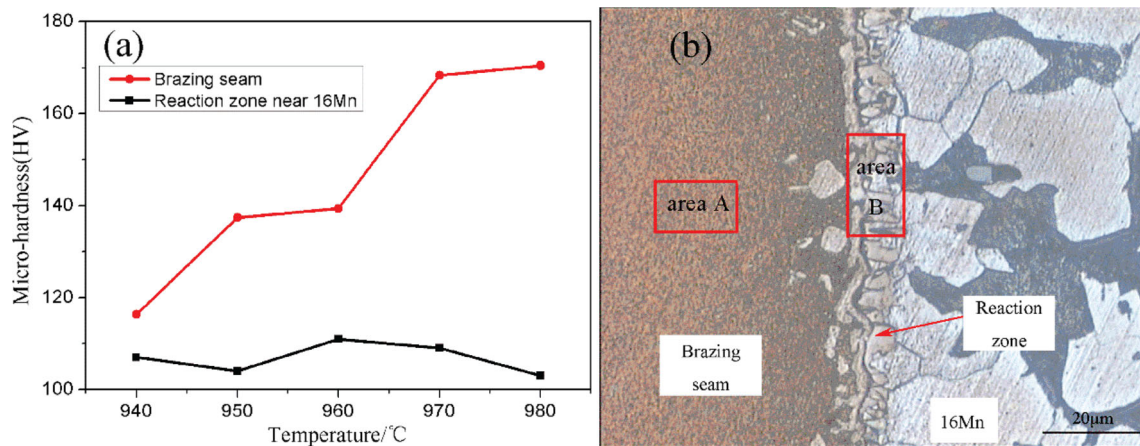


Fig. 8 (a) The result of micro-hardness test for the joints brazed at different temperature and (b) the schematic diagram of testing zone

Table 3 Result of micro-hardness test for the joints (HV)

Temperature/ °C	940	Average	950	Average	960	Average	970	Average	980	Average
Brazing seam	107		102		109		109		102	
	108	107	104	104	111	111	109	109	104	103
	106		105		113		110		103	
Reaction zone near 16Mn	118		138		141		169		171	
	117	117	135	138	140	140	167	169	174	171
	116		141		139		171		168	

occurred at the seams under the temperature 950°C, while near cemented carbide upon the temperature 960°C. This would be due to the wettability and characteristics of Cu-Mn-Zn brazing filler metal at different brazing temperatures. The Cu-Mn-Zn brazing filler metal was very brittle at low temperature, so it was readily to fracture here. And when the temperature was high, the toughness of Cu-Mn-Zn brazing filler metal enhanced owing to the formation of Cu-Zn based solid solution. In addition, the thermal expansion coefficient between Cu-Mn-Zn brazing filler metal and cemented carbide

Table 4 Result of three-point bending test for the joints brazed with CuMnZn brazing filler metal at different brazing temperatures

Temperature (°C)	Bending strength(MPa)	Rupture location
940	497	Brazing seam
950	545	Brazing seam
960	626	Interface near cemented carbide
970	562	Interface near cemented carbide
980	525	Interface near cemented carbide

exist a sharp difference, so it was easy to fracture at the interface near cemented carbide.

The brazing temperature significantly affected the properties of the YG20C/16Mn brazing joints by directly affecting the diffusion of elements and the metallurgical bond strength of joints. With the increase of brazing temperature, the wetting effect of the brazing filler metal on the parent material was enhanced. Thus, the diffusion and dissolution of elements were intensified, and the metallurgical bond strength between the brazing filler metal and the parent material was gradually strengthened. At too high brazing temperature, however, excessive Fe-Co-based solid solution structures were formed at the interfaces, and abundant Cu and Mn were volatilized. Moreover, the plasticity of the seam structures was reduced, and the ability of releasing residual stress by seam structures was weakened. These changes led to the deterioration of the comprehensive mechanical properties of joints. Therefore optimal temperature must be existed when the brazing gap remains 0.20mm. Finally, we got the best temperature 960°C with all the above experiments.

4 Conclusions

- (1) After brazed, the micro-hardness near 16Mn steel was higher than that in brazing seam; the maximum value near 16Mn was 171HV, while it was 111HV in brazing seam.
- (2) Under vacuum conditions, when Cu-Mn-Zn brazing filler metal was used to braze the YG20C cemented carbide with the 16Mn steel, compact structures and very ideal brazing joints without defects such as slag or holes were formed. And the bending strength was up to 626 MP at the temperature of 960°C, which was enhanced by 20.5% compared the bending strength at 940°C.
- (3) Fe-Co-based solid solution was formed in the interface of base materials and brazing seam. When the brazing temperature was high, Co would form excessive Fe-Co-based solid solution structures at the interfaces, reducing the strength of the joints.

Acknowledgment The author gratefully acknowledge the financial support from the Funded by National Natural Science Foundation (51304198), Natural Science Foundation of Jiangsu Province (2013106; 20141134; 2014028-08) and Innovation project for postgraduate (SJLX15_0707)

Reference

1. Chen H, Feng K, Wei S, et al. (2012) Microstructure and properties of WC-Co/3Cr13 joints brazed using Ni electroplated interlayer [J]. *Int. Journal of Refractory Metals and Hard Materials* 33:70–74
2. Chen H, Feng K, Xiong J, et al. (2013) Characterization and stress relaxation of the functionally graded WC-Co/Ni component/stainless steel joint [J]. *Journal of Alloys and Compounds* 557:18–22
3. Zhu L, Luo L, Luo J, et al. (2012) Effect of electroless plating Ni-Cu-P layer on brazability of cemented carbide to steel [J]. *Surface & Coatings Technology* 206:2521–2524
4. Guoqing C, Binggang Z, Zhenzhong W (2013) Electron beam welding-brazing of hard alloy to steel with Ni-Fe intermediate [J]. *Int Journal of Refractory Metals and Hard Materials* 40:58–63
5. Yaoita S, Watanabe T, Sasaki T (2013) Effects of Ni and Co elements in filler metal in Ag brazing of cemented carbide [J]. *Materials Research Innovations* 17(2):142–147
6. Mendez PF, Barnes N, Bell K, et al. (2014) Welding processes for wear resistant overlays [J]. *Journal of Manufacturing Processes* 16: 4–25
7. Yang TE, Yang L, Xiong J, et al. (2014) Brazing behavior of ultra-fine cemented carbide with stainless steel [J]. *Journal of Central South University* 21:2991–2999
8. Wulf E, Bacmann H, Mohwald K, et al. (2014) The influence of brazing temperature and surface roughness on the wettability of reactive brazing alloys [J]. *International Journal of Material Research* 3(105):240–248
9. Joo HG, Lee K (2014) Effect of boron on wear and erosion of WC-Ni vacuum brazed coated [J]. *International Journal of Material Research* 8(105):802–809
10. Akbari Mousavi SAA, Sherafati P, Hoseinion MM (2012) Investigation on Wettability and Metallurgical and Mechanical Properties of Cemented Carbide and Steel Brazed Joint [J]. *Advanced Materials Research* 445:759–764
11. Chunye Z, Hongjie P, Qingfeng L, et al. (2012) Study on the Performance of Brazed Cemented Carbide Cutting Tool [J]. *Advanced Materials Research* 443-444:607–611
12. Nagatsuka K, Sechi Y, Ma N, et al. (2014) Simulation of cracking phenomena during laser brazing of ceramics and cemented carbide [J]. *Science and Technology of Welding and Joining* 8(19):682–688
13. Cai Q, Liu W, Ma Y, et al. (2015) Diffusion brazing of tungsten and steel using Ti-Ni liquid phase forming interlayer [J]. *Fusion Engineering and Design* 91:67–72
14. Gao LX, Zhou T, Zhang DQ, et al. (2014) Microstructure and anodic dissolution mechanism of brazed WC-Ni composite coatings [J]. *Corrosion 204 Engineering, Science and Technology* 3(49): 204–208
15. Yanwei S, Bangsheng L, Aihui L (2010) Evolution of microstructure in centrifugal cast Al-Cu alloy [J]. *CHINA FOUNDRY* 7(1): 43–46
16. Saad N, Lixiao X, Zhou C (2014) Performance of Brazed Carbide End Mill Tool for Machining of Ti6Al4V [J]. *Applied Mechanics and Materials* 541-542:363–367